

## Kinetic Surface Roughening in Molecular Beam Epitaxy of InP

M. A. Cotta, R. A. Hamm, T. W. Staley,<sup>(a)</sup> S. N. G. Chu, L. R. Harriott, and M. B. Panish  
*AT&T Bell Laboratories, Murray Hill, New Jersey 07974*

H. Temkin

*Electrical Engineering Department, Colorado State University, Fort Collins, Colorado 80523*  
 (Received 30 December 1992)

Surface roughening of (100) InP films grown by metalorganic molecular beam epitaxy was observed by scanning force microscopy. The roughening process gives rise to periodic elongated terraces aligned in the  $[0\bar{1}1]$  direction; kinetic control by surface diffusion activation is indicated by the dependence on group III and V fluxes, and growth temperature. Below a given temperature for each set of growth parameters the surface roughness shows two distinct power law regimes dependent on the film thickness. This result supports growth models using ballistic aggregation and surface diffusion.

PACS numbers: 68.55.Bd, 61.16.Ch, 68.35.Bs

To achieve abrupt and planar interfaces in semiconductor structures grown by molecular beam epitaxy (MBE) techniques, it is important to examine the growth morphology and correlate it to the growth mechanism. This mechanism usually depends on surface diffusion of atoms to kink sites, which are energetically more favorable to nucleation. The morphology of the epitaxial film is then influenced by deposition rate, which controls the adatom population on the surface, and substrate temperature, which affects the surface diffusion rate of the species. There are thus different forms of kinetic roughening, depending on the relative magnitude of these variables. In particular, at low temperatures, the reduced surface mobility can lead to three-dimensional growth, where islands nucleate on incomplete monolayers. Recently, there has been considerable theoretical interest in surface roughness and growing interfaces. In particular, scaling behavior of the interface width—or surface roughness,  $W \equiv [(\langle h - \langle h \rangle)^2]^{1/2}$ , where  $h$  is the film thickness—is observed in these models. The scaling is expected to be of the form

$$W(L, t) \sim L^\alpha f(t/L^{a/\beta}),$$

where  $f(x) \sim x^\beta$  for  $x \ll 1$  and  $f(x) \rightarrow \text{const}$  for  $x \gg 1$ , for a system with size  $L$  and time  $t$  [1,2]. Different models of growing interfaces have been proposed [2–4] and, although the values for  $\alpha$  and  $\beta$  agree for spatial dimension  $d=2$  (substrate dimension  $d-1$ ), for  $d > 2$  this is not true [1]. Until now, power law scaling of surface roughness in MBE has been observed experimentally only in the case of iron films grown by this technique [5].

Several experiments have been performed to understand the processes controlling semiconductor MBE growth. Scanning tunneling microscopy of submonolayer growth of Si on Si(100) has shown that surface diffusion is highly anisotropic [6,7]. The existence of a limiting thickness beyond which the film is not epitaxial, with a growth-rate-dependent activation energy, was observed by transmission electron microscopy (TEM) of Si MBE on Si(100) [8]. From the theoretical point of view, simu-

lations based on the solid-on-solid model [9] showed that the thermally activated nature of surface diffusion determines the limiting thickness and its strong temperature dependence.  $W$  was postulated to build gradually with film thickness up to a saturation value, implying a continuous transition from smooth to rough surfaces. A different model, proposed by Kessler, Levine, and Sander [10], considered ballistic aggregation as the sticking mechanism and surface diffusion (BASD) during MBE growth. Simulations for  $d=2$  dimension, for varying diffusion lengths, show a fairly abrupt transition between two power law regimes for the dependence of  $W$  on  $h$ . The first represents surface diffusion scaling, and the second, along with the subsequent saturation, is described by the Kardar-Parisi-Zhang equation [4]. In addition, the first power law regime, for short growth times, is characterized by an exponent  $\beta \sim 0.25$ , significantly lower than that predicted by other authors [11,12].

So far no experiments have been reported on the dynamical scaling behavior during the growth of crystalline semiconductor films by MBE. We discuss changes in surface morphology of InP grown by metalorganic MBE (MOMBE) and show that surface roughening is a kinetically limited phenomenon. Using scanning force microscopy we observe a discontinuous buildup of roughness with film thickness. For each set of growth parameters, there is a minimum temperature where smooth, two-dimensional growth can be obtained. The behavior of  $W$  with  $h$ , at temperatures lower than this minimum, agrees with the predictions of the BASD model [10].

MOMBE, unlike elemental source MBE, involves chemical reactions and catalysis of species on the surface during growth. In MOMBE, the growth rate  $R$  depends on temperature, due to changes in the cracking of metalorganics on the surface of evaporation of species [13]. However, the range of temperatures used in this study provided  $R$  constant with temperature for each set of group III and V fluxes used. This is the region where MOMBE most closely resembles MBE.

The samples were grown on nominal (100) InP sub-

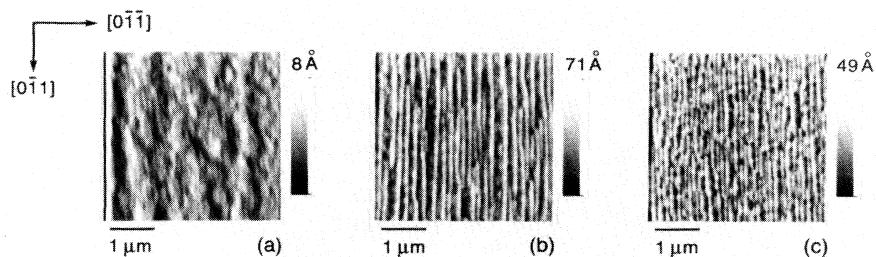


FIG. 1.  $4 \times 4 \mu\text{m}^2$  SFM pictures of 300 nm thick films grown with  $R$ : (a) 1.4  $\text{\AA}/\text{s}$ ; (b) 2.2  $\text{\AA}/\text{s}$ ; and (c) 4.6  $\text{\AA}/\text{s}$  ( $T = 505^\circ\text{C}$ ), determined by varying the TMI flux. The gray scale indicates the height variation in the figure.

strates using trimethylindium (TMI) and phosphine ( $\text{PH}_3$ ) as group III and V sources, respectively. A low-pressure cracking cell provided exclusively  $\text{P}_2$  as the group V precursor. The substrate temperature was measured by a thermocouple immersed in In in a hole at the back of the sample holder, assuring excellent temperature control and reproducibility [14]. Before growth, the substrate was heat treated to  $550^\circ\text{C}$  for  $\sim 20$  s under a  $\text{P}_2$  flux and rapidly returned to the growth temperature. The rms roughness of these heat-treated surfaces was  $W \sim 0.3\text{--}0.5 \text{\AA}$ . The samples were scanned in air with a scanning force microscope (SFM), using high aspect ratio (3:1) Si tips with a radius of  $\sim 5$  nm. Subsequent annealing of the grown samples at growth temperature, under  $\text{P}_2$  flux, did not change the surface morphology.

Figure 1 shows the surface morphologies of 300 nm thick films grown with different growth rates  $R$ . The roughness increases with  $R$  and the surface evolves from a smooth, two-dimensional growth to a pattern with elongated structures along the  $[0\bar{1}1]$  direction, the structures in Fig. 1(b) being more uniform and widely separated than those in Fig. 1(c). Values of  $R$  smaller than that in Fig. 1(a) produce smooth surfaces. The formation of periodic structures for larger values of  $R$  is also observed in the TEM of InP films grown with InGaAs marker layers (Fig. 2). This multilevel system of terraces agrees in depth and profile with the cross section of the SFM pictures. We thus believe that tip convolution effects in the narrow trenches are negligible. Such a system of terraces has been observed *in situ* in GaAs MBE growth on nominal GaAs substrates [15]. This kind of morphology could be expected if any anisotropy along the two perpendicular crystallographic directions is reflected in the rates of the kinetic processes taking place on the surface during growth.

We have observed that increasing the  $\text{P}_2$  flux, or  $R$ , increases  $W$ . These changes result in less time for the molecules to migrate on the surface [16], and indicate that the diffusion process is in the origin of the different morphologies observed. Ghaisas and Das Sarma [17] have shown that the diffusion length depends on the ratio of deposition rate (here the growth rate  $R$ , since  $R$  is constant with temperature) to atomic hopping rate at the growth front. The shapes observed in Fig. 1 would then

come from anisotropic diffusion of the In species along the two crystallographic directions. In the temperature range used here, and from the similarities between InGaAs growth by MBE [18] and MOMBE [19], we believe that the main species migrating on the InP surface is elemental In. Considering the hopping rate as an exponential function of temperature, with an activation energy dependent on the number of lateral bonds [17] the group III atom forms along the two directions (three bonds for the  $[0\bar{1}1]$  step and two bonds for the  $[011]$  step), we expect a smaller value for the  $[0\bar{1}1]$  direction. Based on the ratio of  $W$  along these two directions on surfaces like that shown in Fig. 1(b), a factor of  $\sim 3$  is suggested for the anisotropy of the In diffusion coefficient on the InP surface. This value is close to that measured for Ga on GaAs surfaces [20].

If anisotropic diffusion is involved in the formation of the morphologies observed and the surface roughening, we expect to see similar changes when the temperature is varied. Figure 3 shows the variation of  $W$  along the  $[0\bar{1}1]$  direction with growth temperature for 300 nm thick InP films.  $W$  was measured in one-dimensional cross sections of the surface due to the anisotropy in the

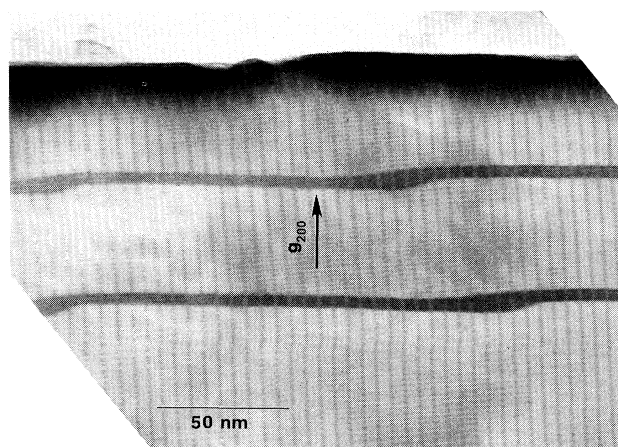


FIG. 2.  $[0\bar{1}1]$  cross section TEM of InP film with elongated structures along the  $[011]$  direction, grown with InGaAs marker layers (dark).

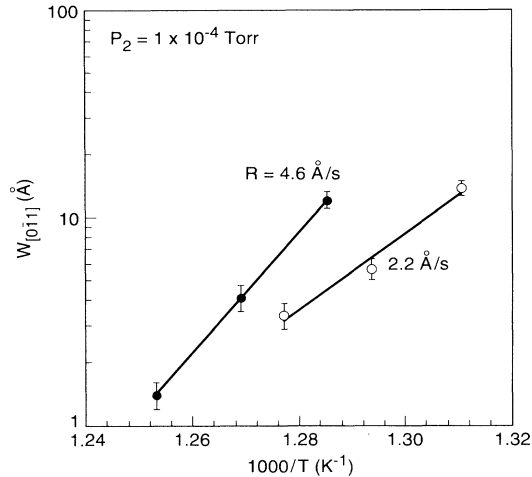


FIG. 3. Temperature dependence of rms roughness  $W$  along the  $[0\bar{1}1]$  direction, for different  $R$ .  $W$  was measured on 1–2  $\mu\text{m}$  long cross sections of the surface.

roughening process. We see in Fig. 3 that  $W$  is indeed temperature activated, increases more rapidly for samples grown with higher growth rates, and vanishes at finite growth temperatures. The latter points to the existence of a minimum growth temperature, for each set of parameters, where two-dimensional growth begins to take place. When varying only the film thickness, at temperatures lower than this minimum, we observe an evolution of surface roughness (Fig. 4), with morphologies very similar to those shown in Fig. 1. A smooth surface evolves into a pattern with elongated terraces aligned in the  $[0\bar{1}1]$  direction. As thickness increases, roughness also builds up along the  $[0\bar{1}1]$  direction, leading eventually to surfaces with isotropic, grainlike structures (not shown). Images of these surfaces show the same height scale as Fig. 4(d), although  $W$  still increases due to the roughening along the  $[0\bar{1}1]$  direction. The similar morphologies observed by decreasing growth temperature or increasing group III flux point to a strong roughening dependence on surface diffusion, its anisotropy reflecting the anisotropy of the kinetic rates.

The elongated structures represent one step in the roughness evolution from a flat to a grainlike surface; the

formation of such structures is likely related to facet formation [21], which can be observed in the TEM (Fig. 2) of our samples. The development of different facets near crystal edges is commonly observed in the epitaxy on patterned substrates;  $\{411\}$  planes usually develop during the growth on patterned (100) substrates for edges aligned in the  $[0\bar{1}1]$  direction [22–24]. These planes are characterized by angles close in value to those observed in our samples for this same crystallographic direction, indicating that these phenomena can be related. While the driving mechanism to the formation of the elongated structures is yet unclear, the overall morphology observed in these samples is not greatly affected by the density of steps on the surface. Some of the growths were carried out on vicinal and nominal (100) InP surfaces simultaneously; the elongated structures are present in both substrates, although  $W$  is higher in the vicinal surfaces [25].

Figure 5 shows  $W$  as a function of the film thickness for samples grown at different temperatures and the same growth rate. We observe that at 520°C  $W$  increases slowly with thickness, and seems to saturate when  $h \sim 1$ –2  $\mu\text{m}$ . At 510°C, there is a sudden increase of  $W$  with  $h$  between 100 and 300 nm, but for  $h$  values below or above this interval, power law regimes can be observed. At 500°C, the roughness builds up very rapidly at the beginning of the growth, the surface showing grainlike structures, but a power law regime again sets in for films thicker than 30 nm, with an exponent ( $\beta \sim 0.1$ ) close to that observed for  $h \geq 300$  nm at 510°C.

Figure 5 provides the opportunity of comparing our experimental results with the BASD model. Kessler, Levine, and Sander [10] calculated the interface width  $W$  as a function of film thickness for varying lengths of a diffusion step. In Fig. 5 we plot  $W$  as a function of film thickness for different growth temperatures. Since surface diffusion, and the corresponding diffusion length, increase with substrate temperature, a qualitative comparison between experiment and theory seems appropriate. We can then see that the predicted transition between two power law regimes [10] is clearly observed in our samples. Also, the length of the first power law regime increases with growth temperature and, consequently, with the diffusion length. The power law exponent observed for the samples grown at 520°C and at 510°C, in

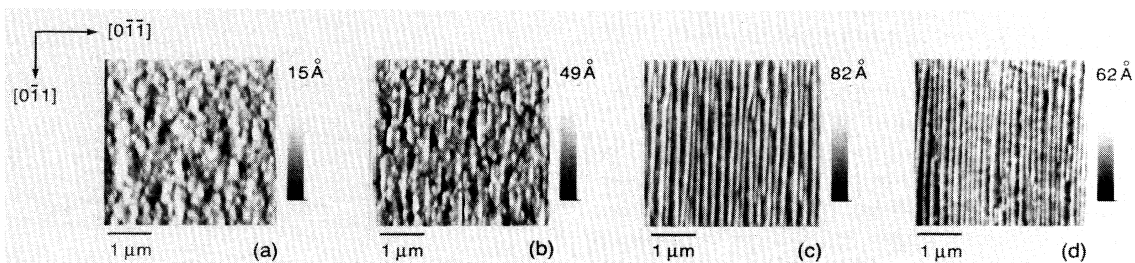


FIG. 4.  $4 \times 4 \mu\text{m}^2$  SFM pictures of films grown under the same conditions ( $R = 4.6 \text{ \AA/s}$ ;  $T = 510^\circ\text{C}$ , and  $P_2$  flux 3 times greater than that in Fig. 1) and different thicknesses: (a) 100 nm; (b) 300 nm; (c) 1  $\mu\text{m}$ ; (d) 2  $\mu\text{m}$ .

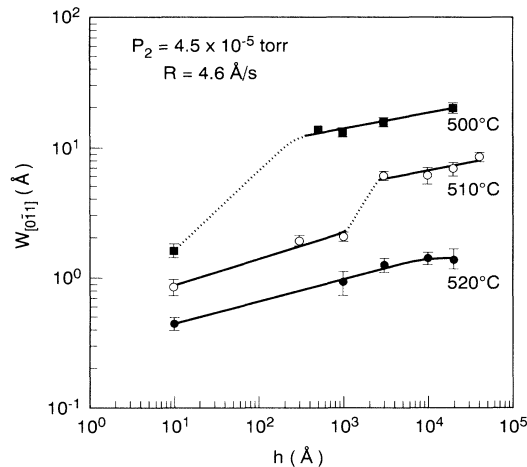


FIG. 5. Dependence of rms roughness  $W$  along the  $[0\bar{1}1]$  direction on the film thickness  $h$  as a function of growth temperature.  $W$  was measured on 1–2  $\mu\text{m}$  long cross sections of the surface.

the range  $h \sim 1\text{--}100$  nm, is  $\beta \sim 0.2$ , close to the value predicted by the BASD model [10]. However, a quantitative comparison of exponents is difficult since the theoretical simulation is carried out for a  $d=2$  dimension. Also, we cannot rule out effects due to the limit on the SFM lateral resolution.

We would like to stress that our results are very different from the limiting thickness for an amorphous-crystalline transition observed by Eaglesham, Gossman, and Cerullo [8] for low temperature Si MBE. Although we observe an evolution of the roughness to that characteristic of three-dimensional growth, the material obtained is of good crystal quality. No significant difference is observed in the bulk electrical or optical properties of InP films grown with different morphologies. The effect of roughness could only be observed in optical measurements of quantum wells.

In summary, we have observed the existence of a roughness buildup on the surface of MOMBE-grown InP films. The same evolution of morphology was observed with changes in group III and V fluxes and growth temperature, indicating a kinetic control by surface diffusion. The ratio between roughness along  $[0\bar{1}\bar{1}]$  and  $[0\bar{1}1]$  directions suggests a factor of  $\sim 3$  for the anisotropy of the In diffusion coefficient along these two directions on InP surface. The qualitative dependence of roughness on film thickness and the observed transition between two power law regimes give support to the BASD model of Kessler, Levine, and Sander [10].

One of the authors (M.A.C.) acknowledges financial

support from CANES/CnPq (Brazil) during this work.

(a)Present address: Materials Science Program, University of Wisconsin-Madison, Madison, WI 53706.

- [1] J. G. Amar and F. Family, Phys. Rev. A **41**, 3399 (1990).
- [2] F. Family and T. Vicsek, J. Phys. A **18**, L75 (1985).
- [3] J. Kertész and D. E. Wolf, J. Phys. A **21**, 747 (1988).
- [4] M. Kardar, G. Parisi, and Y. Zhang, Phys. Rev. Lett. **56**, 889 (1986).
- [5] J. Chevrier, V. LeThanh, R. Buys, and J. Derrien, Europhys. Lett. **16**, 732 (1991).
- [6] Y.-W. Mo, B. S. Swartzentruber, R. Kariotis, M. B. Webb, and M. G. Lagally, Phys. Rev. Lett. **63**, 2393 (1989).
- [7] Y.-W. Mo, J. Kleiner, M. B. Webb, and M. G. Lagally, Phys. Rev. Lett. **66**, 1998 (1991).
- [8] D. J. Eaglesham, H.-J. Gossman, and M. Cerullo, Phys. Rev. Lett. **65**, 1227 (1990).
- [9] S. Das Sarma and P. I. Tamborenea, Phys. Rev. B **46**, 1925 (1992).
- [10] D. A. Kessler, H. Levine, and L. M. Sander, Phys. Rev. Lett. **69**, 100 (1992).
- [11] S. Das Sarma and P. Tamborenea, Phys. Rev. Lett. **66**, 325 (1991).
- [12] D. Wolf and J. Villain, Europhys. Lett. **13**, 389 (1990).
- [13] J. Ch. Garcia, Ph. Maurel, Ph. Bove, and J. P. Hirtz, J. Appl. Phys. **69**, 3297 (1991).
- [14] R. A. Hamm, D. Ritter, H. Temkin, M. B. Panish, J. M. Vandenberg, and R. D. Yadvish, Appl. Phys. Lett. **59**, 1893 (1991).
- [15] E. J. Heller and M. G. Lagally, Appl. Phys. Lett. **60**, 2675 (1992).
- [16] M. Hata, A. Watanabe, and T. Isu, J. Cryst. Growth **111**, 83 (1991).
- [17] S. V. Ghaisas and S. Das Sarma, Phys. Rev. B **46**, 7308 (1992).
- [18] D. J. Arent, S. Nilsson, Y. D. Galeuchet, H. P. Meier, and W. Walter, Appl. Phys. Lett. **55**, 2611 (1989).
- [19] M. A. Cotta, L. R. Harriott, Y. L. Wang, R. A. Hamm, H. H. Wade, J. S. Weiner, D. Ritter, and H. Temkin, Appl. Phys. Lett. **61**, 1936 (1992).
- [20] K. Ohta, T. Kojima, and T. Nakagawa, J. Cryst. Growth **95**, 71 (1989).
- [21] R. J. Phaneuf, E. D. Williams, and N. C. Bartelt, Phys. Rev. B **38**, 1984 (1988).
- [22] M. A. Cotta, R. A. Hamm, T. W. Staley, R. D. Yadvish, L. R. Harriott, and H. Temkin, Appl. Phys. Lett. **62**, 496 (1993).
- [23] W. T. Tsang and A. Y. Cho, Appl. Phys. Lett. **30**, 293 (1977).
- [24] F. S. Turco, M. C. Tamargo, D. M. Hwang, R. E. Nahory, J. Werner, K. Kash, and E. Kapon, Appl. Phys. Lett. **56**, 72 (1990).
- [25] M. A. Cotta, R. A. Hamm, T. W. Staley, L. R. Harriott, and H. Temkin (unpublished).

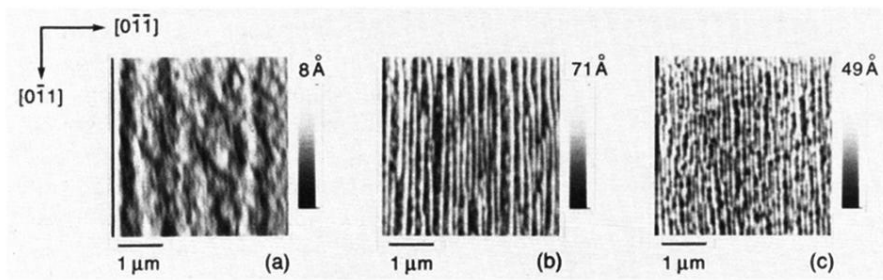


FIG. 1.  $4 \times 4\ \mu\text{m}^2$  SFM pictures of 300 nm thick films grown with  $R$ : (a)  $1.4\ \text{\AA}/\text{s}$ ; (b)  $2.2\ \text{\AA}/\text{s}$ ; and (c)  $4.6\ \text{\AA}/\text{s}$  ( $T = 505^\circ\text{C}$ ), determined by varying the TMI flux. The gray scale indicates the height variation in the figure.

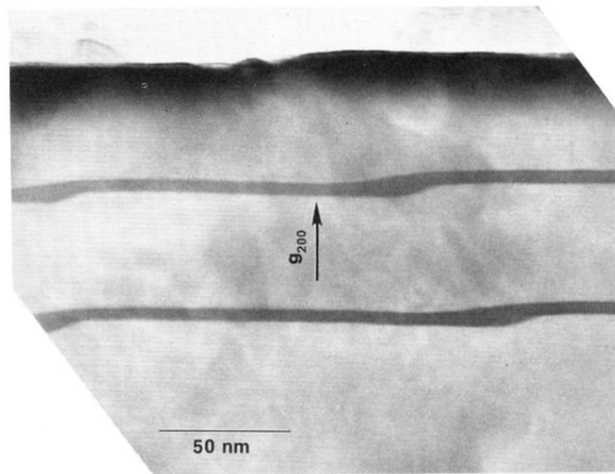


FIG. 2.  $[0\bar{1}1]$  cross section TEM of InP film with elongated structures along the  $[0\bar{1}1]$  direction, grown with InGaAs marking layers (dark).

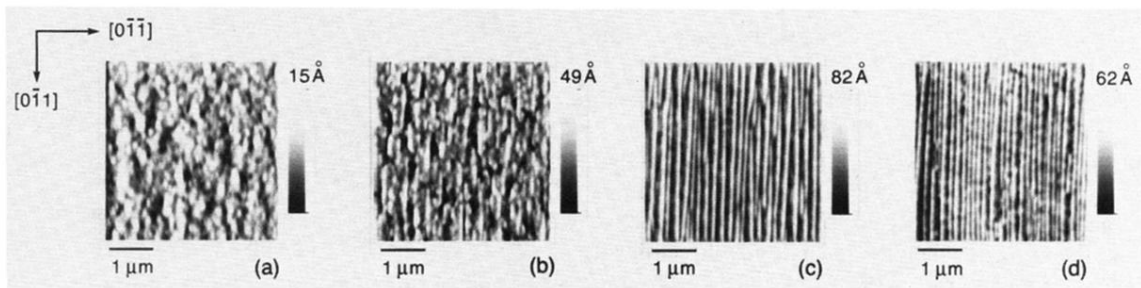


FIG. 4.  $4 \times 4 \mu\text{m}^2$  SFM pictures of films grown under the same conditions ( $R=4.6 \text{ \AA}/\text{s}$ ;  $T=510^\circ\text{C}$ , and  $\text{P}_2$  flux 3 times greater than that in Fig. 1) and different thicknesses: (a) 100 nm; (b) 300 nm; (c)  $1 \mu\text{m}$ ; (d)  $2 \mu\text{m}$ .